

# Unsteady motion of two-dimensional dipole in water under floating compressed elastic plate

Yury A. Stepanyants<sup>1,2</sup> and Izolda V. Sturova<sup>3</sup>

<sup>1</sup>School of Sciences, University of Southern Queensland, Toowoomba, QLD, 4350, Australia

<sup>2</sup>Department of Applied Mathematics, Nizhny Novgorod State Technical University, Nizhny Novgorod, 603950, Russia

<sup>3</sup>Lavrentyev Institute of Hydrodynamics of SB RAS, Novosibirsk, 630090, Russia

\*E-mail address of the presenting author: sturova@hydro.nsc.ru

## 1 Introduction

The velocity potential of a transient source of arbitrary strength and in arbitrary two-dimensional motion is derived, wherein a thin elastic plate of infinite extent is assumed to cover the surface of water. This potential is fundamental in the analysis of flexural-gravity waves (FGW) generation by various types of motion of a submerged body. As a simple application, the potential of a point dipole is considered; this models the unsteady horizontal motion of a circular cylinder perpendicular to its axis. Das et al. (2018) investigated the propagation of FGW including the effect of compression and current. The purpose of this work is to study the properties of FGW arising from the superposition of the translating and oscillating dipole motion.

## 2 Mathematical formulation

Consider a fixed rectangular coordinate system  $Oxy$ , where the  $x$ -axis coincides with the unperturbed upper boundary of water, and positive direction of the  $y$ -axis is upward. A water of the constant density  $\rho$  and uniform depth  $H$  is assumed to be incompressible and inviscid, and its motion is assumed to be potential. The upper boundary of water is covered with a thin elastic plate. This model is used to analyze floating ice sheets and very large floating structures (e.g., platforms). It is assumed that the water motion occurs in the result of the action of a point mass source of a variable intensity; the source turns on at the time  $t = 0$ . The source position at  $t \geq 0$  is determined by its trajectory  $\boldsymbol{\xi} = (\xi(t), \eta(t))$  and the intensity  $\mu(t)$ , where  $-H < \eta(t) < 0$  and  $\mu(t) = 0$  for  $t < 0$ . There exists a velocity potential  $\Phi(x, y, t)$  which satisfies the Poisson equation:

$$\Delta\Phi = \mu(t)\delta(\mathbf{x} - \boldsymbol{\xi}(t)), \quad (|x| < \infty, -H \leq y \leq 0). \quad (1)$$

Here  $\Delta$  denotes the two-dimensional Laplace operator in the  $(x, y)$ -plane,  $\mathbf{x} = (x, y)$ , and  $\delta$  is the Dirac delta-function.

Then we assume that the lower boundary of the elastic plate is always in a contact with the water. Denoting by  $w(x, t)$  the elastic plate deflection, the linearized kinematic and dynamic boundary conditions are given by (see, e.g., Kheysin (1967)):

$$\partial w / \partial t = \partial \Phi / \partial y, \quad D \partial^4 w / \partial x^4 + Q \partial^2 w / \partial x^2 + M \partial^2 w / \partial t^2 + \rho \partial \Phi / \partial t + \rho g w = 0 \quad (y = 0), \quad (2)$$

where  $D = Eh_1^3 / [12(1 - \nu^2)]$ ,  $M = \rho_1 h_1$ ;  $E$ ,  $\nu$ ,  $\rho_1$ ,  $h_1$  are the Young modulus, the Poisson ratio, the density and thickness of the elastic plate;  $Q$  is the longitudinal stress ( $Q > 0$  corresponds to compression, and  $Q < 0$  to stretching);  $g$  is the acceleration due to gravity. The bottom is assumed non-permeable, so that

$$\partial \Phi / \partial y = 0 \quad (y = -H). \quad (3)$$

It is assumed that far from the source water is calm and the velocity field tends to zero for all  $t > 0$ :

$$\lim_{r \rightarrow \infty} \nabla \Phi = 0 \quad (t \geq 0), \quad r = |x - \xi(t)|. \quad (4)$$

The initial conditions at  $y = 0$  and all  $x$  are:

$$\Phi = w = \partial w / \partial t = 0 \quad (t = 0). \quad (5)$$

To solve the initial-boundary problem (1)–(5), we use the Laplace and Fourier transforms:

$$\hat{\Phi}(k, y, s) = \int_0^\infty e^{-st} \int_{-\infty}^\infty \Phi(x, y, t) e^{-ikx} dx dt \quad (6)$$

with  $\text{Re } s > 0$  and real  $k$ .

Our main interest in this problem is the determination of the elastic plate deflection  $w(x, t)$ . The Laplace and Fourier transforms of function  $w(x, t)$  can be found from the formula  $\hat{w}(k, s) = \hat{\Phi}'(k, 0, s)/s$  which follows from the first of Eqs. (2). Using then Eqs. (1)–(6) to determine  $\hat{\Phi}'(k, 0, s)$ , we ultimately find:

$$\hat{w} = \frac{\rho s}{B(k)[s^2 + \omega^2(k)] \cosh(kH)} \int_0^\infty \mu(t) e^{-st - ik\xi(t)} \cosh[k(H + \eta(t))] dt,$$

where  $B(k) = \rho + kM \tanh(kH)$ , and the dispersion relation for the linear FGW is:

$$\omega(k) = \sqrt{\frac{k(Dk^4 - Qk^2 + \rho g)}{\rho \coth(kH) + kM}}. \quad (7)$$

The plate deformation in the real  $(x, t)$ -space can be obtained by means of the inverse Fourier and Laplace transforms of  $\hat{\Phi}(k, y, s)$ , and the final formula for the function  $w(x, t)$  is:

$$w(x, t) = \frac{\rho}{\pi} \int_0^\infty \frac{dk}{B(k) \cosh(kH)} \int_0^t \mu(\tau) \cos[k(x - \xi(\tau))] \cos[\omega(k)(t - \tau)] \cosh[k(H + \eta(\tau))] d\tau.$$

The simplest example of a submerged body that can be modeled by point sources in the two-dimensional case is a circular cylinder. The motion of such a cylinder is simulated by a dipole with the moment  $\mathbf{M}(t) = M_0 \mathbf{U}(t)$ , where  $M_0 = 2\pi R^2$ ,  $\mathbf{U} = (U_1, U_2) = d\boldsymbol{\xi}(t)/dt$ ,  $\mathbf{x} = \boldsymbol{\xi}(t)$  is the trajectory of the cylinder center, and  $R$  is its radius.

Solution for vertical displacement of the elastic plate caused by the motion of a dipole has the form:

$$w(x, t) = \frac{\rho M_0}{\pi} \int_0^\infty \frac{k dk}{B(k) \cosh kH} \int_0^t \left\{ U_1(\tau) \sin[k(x - \xi(\tau))] \cosh[k(H + \eta(\tau))] + U_2(\tau) \cos[k(x - \xi(\tau))] \sinh[k(H + \eta(\tau))] \right\} \cos[\omega(k)(t - \tau)] d\tau. \quad (8)$$

Further, we restrict ourselves by consideration the dipole moving only in the horizontal direction at a fixed depth  $h$  and set  $U_2(t) = 0$ ,  $\eta(t) = -h$ .

### 3 Horizontally moving and oscillating dipole

Assume that a dipole instantly accelerates from zero to a constant speed  $U_0$  and periodically oscillates with the constant amplitude  $\gamma$  and frequency  $\Omega$ , so that its trajectory has the form:

$$\xi(t) = U_0 t + \gamma \sin \Omega t, \quad U_1(t) = U_0 + \gamma \Omega \cos \Omega t.$$

In the moving coordinate frame  $X = U_0 t - x$ , solution (8) can be written as:

$$w(X, t) = \frac{\rho M_0}{\pi} \int_0^\infty \frac{k \cosh[k(H - h)]}{B(k) \cosh kH} \int_0^t (U_0 + \gamma \Omega \cos \Omega \tau) \times \sin\{[k(U_0(t - \tau) - X - \gamma \sin \Omega \tau)]\} \cos[\omega(k)(t - \tau)] d\tau dk.$$

For small amplitude oscillations of the dipole this formula can be further linearized with respect to  $\gamma$  and presented in the form:

$$w(X, t) = w_0(X, t) + \gamma [W_c(X, t) \cos \Omega t + W_s(X, t) \sin \Omega t], \quad (9)$$

where function  $w_0(X, t)$  describes purely horizontally motion of dipole with a constant speed  $U_0$  without oscillation:

$$w_0(X, t) = \frac{\rho M_0 U_0}{2\pi} \int_0^\infty \frac{k \cosh[k(H - h)]}{B(k) \cosh kH} [I_c(k) \cos kX - I_s(k) \sin kX] dk.$$

Here the following notations were introduced:

$$I_c(k) = \sum_{n=1}^2 \frac{1 - \cos [(U_0 k + (-1)^n \omega(k))t]}{U_0 k + (-1)^n \omega(k)}, \quad I_s(k) = \sum_{n=1}^2 \frac{\sin [(U_0 k + (-1)^n \omega(k))t]}{U_0 k + (-1)^n \omega(k)},$$

and functions  $W_c(X, t)$  and  $W_s(X, t)$  are defined by the formulae:

$$(W_c, W_s) = \frac{\rho M_0 \Omega}{\pi} \int_0^\infty \frac{k \cosh [k(H - h)]}{B(k) \cosh kH} \int_0^t (\cos \Omega p, \sin \Omega p) \sin [k(U_0 p - X)] \cos [\omega(k)p] dp dk. \quad (10)$$

Solution (9) allows us to determine the vertical deflection of elastic plate at any time.

To study the behavior of functions  $W_c$  and  $W_s$  in the far-field zone when  $|X|, t \rightarrow \infty$ , we use the method of stationary phase which allows us to estimate asymptotically the double integrals (10). The phase functions in these integrals are:

$$\Psi_{1,2}(k, p) = k(U_0 p - X) \pm p[\Omega + \omega(k)], \quad \Psi_{3,4}(k, p) = k(U_0 p - X) \pm p[\Omega - \omega(k)]. \quad (11)$$

The stationary points are solutions of the following set of simultaneous equations:

$$\partial \Psi_i / \partial k = 0 \quad \rightarrow \quad d\omega/dk = \pm (U_0 - X/p), \quad \partial \Psi_i / \partial p = 0 \quad \rightarrow \quad \omega/k = \pm \Omega/k \pm U_0.$$

As well-known, the dispersion relation (7) for FGW imposes a restriction on the maximal value of a compression force. The stability of oscillations of a floating ice plate is guaranteed by the condition  $Q < Q_* \equiv 2\sqrt{g\rho D}$ , whereas at  $Q > Q_*$  the ice plate shatters (see, e.g., Kheisin (1967), Bukatov (2017), Das et al. (2018)). There is one more critical value of the parameter  $Q$  such that for  $Q < Q_0 < Q_*$ , the group velocity of FGW  $c_g = d\omega/dk$  is positive for all wavenumbers  $k \geq 0$ . Such a case when  $c_g > 0$  will be dubbed *the normal dispersion* in contrast to the case of *anomalous dispersion* when  $Q_0 < Q < Q_*$ . The latter case is characterized by the presence of a wavenumber interval within which the group velocity is negative. Both these critical values  $Q_*$  and  $Q_0$ , as well as the corresponding wavenumbers  $k_*$  and  $k_0$  can be determined from the joint solution of two simultaneous equations  $c_g(k) = 0$  and  $dc_g/dk = 0$ .

To determine the stationary points of functions  $\Psi_i(k, p)$  ( $i = 1, \dots, 4$ ) in (11), we restrict ourselves by consideration an infinitely deep fluid, because in this case, the determination of stationary points reduces to the finding of the roots of polynomials, whereas in the case of a fluid of finite depths, it is necessary to solve transcendental equations.

Further we introduce the following dimensionless parameters:

$$\bar{D} = D/(g\rho R^4), \quad \bar{M} = M/(\rho R), \quad \bar{Q} = Q/(g\rho R^2), \quad F = U_0/\sqrt{gR}, \quad (\sigma, \bar{\omega}) = (\Omega, \omega)\sqrt{R/g}, \quad \bar{k} = kR.$$

The dispersion relation (7) in the deep-water limit in the dimensionless variables is:

$$\bar{\omega}(\bar{k}) = \sqrt{\bar{k}(\bar{D}\bar{k}^4 - \bar{Q}\bar{k}^2 + 1)/(1 + \bar{k}\bar{M})}.$$

The analysis of the stationary points behavior in the case of normal dispersion was performed by Sturova (2013). It was shown that function  $\Psi_1$  in Eq. (11) does not have stationary points. The function  $\Psi_2$  has no more than two stationary points, which we denote as  $k_2^{(1)}$  and  $k_2^{(2)}$ . Function  $\Psi_3$  has at most three stationary points  $k_3^{(1)}$ ,  $k_3^{(2)}$ ,  $k_3^{(3)}$ . Function  $\Psi_4$  always has only one stationary point  $k_4^{(1)}$ . The only difference in the case of anomalous dispersion, ( $Q_0 < Q < Q_*$ ), is that function  $\Psi_4$  has at most three stationary points  $k_4^{(1)}$ ,  $k_4^{(2)}$ ,  $k_4^{(3)}$ . Therefore, in the case of normal dispersion, the total number of stationary points does not exceed six, whereas in the case of anomalous dispersion, it does not exceed eight.

The directions of wave propagation which are determined by the stationary points of functions  $\Psi_2$  and  $\Psi_3$  depend on the sign of the expression  $F - \bar{c}_g(k)$ , and for function  $\Psi_4$  the direction depends on the sign of the expression  $F + \bar{c}_g(k)$ . In all these expressions one need to plug the wavenumbers of stationary points corresponding to each function instead of  $k$ . Waves with the positive value of

expressions  $F \pm \bar{c}_g(k)$  propagate downstream ( $X > 0$ ), whereas waves with the negative value of this expressions propagate upstream ( $X < 0$ ).

Fig. 1 shows the partition of the parameter plane ( $\sigma, F$ ) into several domains depending on the number of generated waves. The following input data were used:  $E = 5 \cdot 10^9$  Pa,  $\nu = 0.3$ ,  $\rho_1 = 922.5$  kg/m<sup>3</sup>,  $h_1 = 1$  m,  $\rho = 1025$  kg/m<sup>3</sup>,  $R = 5$  m,  $g = 9.81$  m/s<sup>2</sup>. For these data set we have  $\tilde{Q}_0 \equiv Q_0/\sqrt{g\rho D} = 1.475$ .

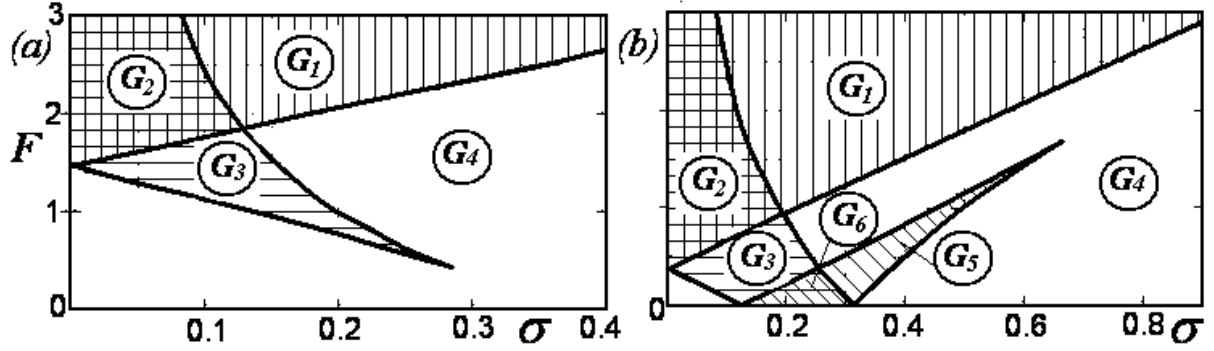


**Figure 1.** The parameter plane partition depending on the number of generated waves for the normal dispersion,  $\tilde{Q} = 1.2$ , (a) and anomalous dispersion (b),  $\tilde{Q} = 1.95$ .

The case of normal dispersion ( $\tilde{Q} \equiv Q/\sqrt{g\rho D} = 1.2$ ) is shown in Fig. 1(a). For the parameters  $\sigma$  and  $F$  from the domain  $G_1$  (marked by vertical hatching), there are four stationary points  $k_2^{(1)}$ ,  $k_2^{(2)}$ ,  $k_3^{(1)}$ ,  $k_4^{(1)}$ , two of which ( $k_2^{(1)}$ ,  $k_4^{(1)}$ ) cause wave perturbations running downstream, and the other two ( $k_2^{(2)}$ ,  $k_3^{(1)}$ ) – running upstream. For the domain  $G_2$  (marked by the combination of horizontal and vertical hatching) there are six stationary points three of which ( $k_2^{(1)}$ ,  $k_3^{(2)}$ ,  $k_4^{(1)}$ ) cause wave perturbations running downstream, and the other three ( $k_2^{(2)}$ ,  $k_3^{(1)}$ ,  $k_3^{(3)}$ ) – running upstream. For the domain  $G_3$  (marked by horizontal hatching) there are four stationary points two of which ( $k_3^{(2)}$ ,  $k_4^{(1)}$ ) cause wave perturbations running downstream, and the other two ( $k_3^{(1)}$ ,  $k_3^{(3)}$ ) – running upstream. For the domain  $G_4$  (no shaded domain) there are only two stationary points, one of which  $k_4^{(1)}$  causes wave perturbation propagating downstream, and another one,  $k_3^{(1)}$ , – running upstream.

The case of anomalous dispersion with  $\tilde{Q} = 1.95$  is shown in Fig. 1(b). In addition to the listed domains  $G_1, \dots, G_4$ , the domains  $G_5$  and  $G_6$  appear in this case. In the domain  $G_5$  (shown by oblique hatching) there are four stationary points two of which ( $k_4^{(1)}$ ,  $k_4^{(3)}$ ) cause wave perturbations running downstream, and the other two ( $k_3^{(1)}$ ,  $k_4^{(2)}$ ) – running upstream. For the domain  $G_6$  (shown by combined horizontal and oblique hatching) there are six stationary points, three of which ( $k_3^{(2)}$ ,  $k_4^{(1)}$ ,  $k_4^{(3)}$ ) cause wave perturbations running downstream, and the other three ( $k_3^{(1)}$ ,  $k_3^{(3)}$ ,  $k_4^{(2)}$ ) – running upstream.

More detailed analysis of theoretical and numerical results will be presented at the Workshop.

## Acknowledgment

The work of Y.S. was supported by the grant number SPARC/2018–2019/P751/SL through the Scheme for Promotion of Academic and Research Collaboration of the Ministry of Human Resource Development, Government of India and the grant number NSH-2685.2018.5 provided by the President of Russian Federation for the State support of leading Scientific Schools of the Russian Federation.

## References

- Bukatov, A.E. 2017 *Waves in a Sea with a Floating Ice Cover (in Russian)*.
- Das, S., Sahoo, T., Meylan, M.H. 2018 Dynamics of flexural gravity waves: from sea ice to Hawking radiation and analogue gravity. *Proc. R. Soc. A*, **474**, 20170223.
- Kheisin, D. Ye. 1967 *Dynamics of Floating Ice Cover (in Russian. Technical English Translation in: FSTC-HT-23-485-69, U.S. Army Foreign Science and Technology Center)*.
- Sturova, I.V. 2013 Unsteady three-dimensional sources in deep water with an elastic cover and their applications. *J. Fluid Mech.*, **730**, 392–418.